J Solid State Electrochem (2002) 7: 30–36
DOI 10.1007/s10008-002-0286-3

ORIGINAL PAPER

**V.V. Kharton · A.V. Kovalevsky · E.V. Tsipis
A.P. Viskup · E.N. Naumovich · J.R. Jurado
J.R. Frade**

Mixed conductivity and stability of A-site-deficient $Sr(Fe,Ti)O_{3-\delta}$ perovskites

Received: 19 February 2002 / Accepted: 27 March 2002 / Published online: 16 May 2002

Abstract Deficiency in the A sublattice of perovskite-type $Sr_{1-y}Fe_{0.8}Ti_{0.2}O_{3-\delta}$ ($y = 0$–0.06) leads to suppression of oxygen-vacancy ordering and to increasing oxygen ionic conductivity, unit cell volume, thermal expansion, and stability in CO_2-containing atmospheres. The total electrical conductivity, predominantly p-type electronic in air, decreases with increasing A-site deficiency at 300–700 K and is essentially independent of the cation vacancy concentration at higher temperatures. Oxygen ion transference numbers for $Sr_{1-y}Fe_{0.8}Ti_{0.2}O_{3-\delta}$ in air, estimated from the faradaic efficiency and oxygen permeation data, vary in the range from 0.002 to 0.015 at 1073–1223 K, increasing with temperature. The maximum ionic conductivity was observed for $Sr_{0.97}Fe_{0.8}Ti_{0.2}O_{3-\delta}$ ceramics. In the system $Sr_{0.97}Fe_{1-x}Ti_xO_{3-\delta}$ ($x = 0.1$–0.6), thermal expansion and electron-hole conductivity both decrease with x. Moderate additions of titanium (up to 20%) in $Sr_{0.97}(Fe,Ti)O_{3-\delta}$ result in higher ionic conductivity and lower activation energy for ionic transport, owing to disordering in the oxygen sublattice; further doping decreases the ionic conduction. It was shown that time degradation of the oxygen permeability, characteristic of $Sr(Fe,Ti)O_{3-\delta}$ membranes and resulting from partial ordering processes, can be reduced by cycling of the oxygen pressure at the membrane permeate side. Thermal expansion coefficients of $Sr_{1-y}Ti_{1-x}Fe_xO_{3-\delta}$ ($x = 0.10$–0.60, $y = 0$–0.06) in air are in the range $(11.7–16.5)\times10^{-6}$ K^{-1} at 350–750 K and $(16.6–31.1)\times10^{-6}$ K^{-1} at 750–1050 K.

Keywords Perovskite · Strontium ferrite · A-site deficiency · Ionic conductivity · Thermal expansion

V.V. Kharton (✉) · E.V. Tsipis · J.R. Frade
Department of Ceramics and Glass Engineering,
CICECO, University of Aveiro, 3810-193 Aveiro, Portugal
E-mail: kharton@cv.ua.pt
Tel.: +351-234-370263
Fax: +351-234-425300

V.V. Kharton · A.V. Kovalevsky · A.P. Viskup
E.N. Naumovich
Institute of Physicochemical Problems,
Belarus State University, 14 Leningradskaya Str.,
220050 Minsk, Republic of Belarus

J.R. Jurado
Institute of Ceramics and Glass,
CSIC, 28500 Arganda del Rey, Madrid, Spain

Introduction

Great interest has been shown in transition metal-containing perovskite-type oxides owing to their ability to stabilize higher oxidation states of 3d transition metal cations and to accommodate large amounts of various dopants and oxygen vacancies, which often provide unique electrical and electrocatalytic properties [1, 2, 3]. Numerous perovskite-like phases have thus been considered for high-temperature electrochemical applications, including oxygen-separation membranes, solid oxide fuel cells (SOFCs), and sensors [1, 2, 3, 4]. One representative group of materials, which exhibit a high mixed oxygen-ionic and electronic conductivity and hence are promising for use in electrochemical devices, relates to the solid solutions based on strontium ferrite, $SrFeO_{3-\delta}$ [5, 6, 7, 8, 9].

In the oxygen-nonstoichiometric $SrFeO_x$ system, the crystal structure and transport properties are considerably affected by oxygen-vacancy ordering [9, 10, 11, 12]. While the stoichiometric end member, $SrFeO_3$, has a disordered cubic perovskite lattice, a series of structurally distinct vacancy-ordered phases is formed with decreasing oxygen partial pressure and oxygen content [11, 12]. The reduction is accompanied with a large volume expansion, which is one important reason for the instability of $SrFeO_{3-\delta}$-based membranes under high oxygen-pressure gradients [5, 6]. Substitution of iron with higher-valence cations, such as Ti^{4+}, enables stabilization of the lattice and to decrease the chemically induced expansion, but leads to a lower ionic conductivity [5, 9, 13, 14, 15].

Another important problem limiting the applicability of the perovskite-type phases containing significant amounts of alkaline-earth cations is their reactivity with

some gases such as CO_2 (for example [16, 17]). This interaction can be partially suppressed by the creation of moderate A-site deficiency [17, 18]. However, the effects of A-site cation vacancies on the oxygen ionic conduction in perovskites are still unclear. For lanthanum-strontium gallates and aluminates, A-site deficiency was found to decrease the ionic conductivity [19, 20, 21]. For cobaltites, (La,Sr)$CoO_{3-\delta}$, the ionic and p-type electronic conductivities both decrease when cation vacancies are created in the A sublattice [22, 23]. On the other hand, oxygen ionic transport in A-site deficient perovskite-type manganites is higher than that in the cation-stoichiometric phases [24, 25].

The present paper continues our study of the Sr(Fe,Ti)$O_{3-\delta}$ system [14, 15, 18, 26, 27], focusing on the effects of A-site deficiency and B-site cation composition on the physicochemical properties of solid solutions with a high iron content. In order to estimate the optimum nonstoichiometry in the A sublattice, particular emphasis is given to the relationships between A-site vacancy concentration, ionic conductivity, thermal expansion, and stability with respect to interaction with carbon dioxide. Another important goal was to evaluate the influence of cycling the oxygen pressure on the oxygen permeability of Sr(Fe,Ti)$O_{3-\delta}$ membranes. Owing to partial ordering in the oxygen sublattice, typical for $SrFeO_{3-\delta}$-based materials [9, 10], the Ti-containing strontium ferrites exhibit a relatively fast degradation of ionic transport with time [14, 15]. Cycling of the oxygen partial pressure at the permeate side of $SrCo_{1-x}Ti_xO_{3-\delta}$ membranes was found to suppress time degradation [28]; a similar effect might also be expected in the case of Sr(Fe,Ti)$O_{3-\delta}$ ceramics.

Experimental

Single-phase powders of $Sr_{1-y}Fe_{1-x}Ti_xO_{3-\delta}$ ($x = 0.10$–0.40, $y = 0$–0.06) were synthesized using a standard ceramic technique from the stoichiometric amounts of high-purity $SrCO_3$, TiO_2, $FeC_2O_4{\cdot}2H_2O$, or Fe_3O_4. The solid-state reactions were performed at 1270–1470 K for 35 h in air with multiple intermediate regrindings. Formation of single perovskite phases was verified by X-ray diffraction (XRD) analysis. The bar- ($4\times4\times30$ mm^3) and disk-shaped (diameter of 10–20 mm) samples were compacted at 300–500 MPa, and then sintered in air at 1470–1670 K during 4–20 h. After sintering, the ceramics were slowly cooled (3 K/min) to room temperature, in order to obtain equilibrium oxygen nonstoichiometry. The density of the sintered ceramic samples was not less than 93% of their theoretical density, calculated from XRD results.

Characterization of the ceramic materials included XRD, infrared (IR) absorption spectroscopy, scanning electron microscopy combined with energy dispersive spectroscopy (SEM/EDS), dilatometry, and measurement of total electrical conductivity by the four-probe DC method. Chemical composition of selected samples was confirmed by ion-coupled plasma (ICP) spectroscopic analysis, which showed the deviation of the cation compositions from the formulas to be less than 0.2 at%. The total content of the impurities was found to be less than 0.1 at%, comparable with the detection limit. Experimental techniques and equipment used for the characterization have been described elsewhere (see [14, 15, 18, 22, 23, 24, 26, 27, 28, 29] and references therein).

The oxygen ion transference numbers and ionic conductivity values were calculated from the results of oxygen permeability (OP), faradaic efficiency (FE), and total conductivity measurements, as described earlier [14, 15, 26]. Detailed description of the experimental procedures for the determination of steady OP fluxes and FE can be found elsewhere [22, 26, 28, 29]. For all results on the OP presented in this paper, the membrane feed-side oxygen pressure (p_2) was maintained at 21 kPa (atmospheric air), whilst the oxygen partial pressure at the membrane permeate side (p_1) was varied from 1 Pa to 21 kPa. The FE results were obtained under the oxygen partial pressures of 21 kPa at both sides of the ceramic membranes.

Most of the $Sr_{1-y}Fe_{1-x}Ti_xO_{3-\delta}$ ceramics showed an extremely prolonged process of steady-state attainment after placing them under an oxygen chemical potential gradient in cells for OP measurements. This behavior has been analyzed elsewhere [15, 26]. During the first application of an oxygen chemical potential gradient across the sample, the oxygen flux slowly decreased for as long as 100–700 h. Subsequent measurements required much shorter transient times (3–25 h). A criterion for steady-state attainment was thus defined as the time independence of the flux during 20–25 h, within the standard experimental error limits. All data on steady OP, presented below, were obtained using this condition. In the case of FE measurements under a zero oxygen chemical potential gradient, steady-state attainment required times in the range 5–40 h.

Results and discussion

Phase composition and structure

XRD analysis demonstrated that all powders and ceramics of $Sr_{1-y}Fe_{0.8}Ti_{0.2}O_{3-\delta}$ ($y = 0.01$–0.06) and $Sr_{0.97}Fe_{1-x}Ti_xO_{3-\delta}$ ($x = 0.10$–0.40) were single phase. The crystal lattice was identified as a cubic perovskite-type. The only exception was the A-site stoichiometric compound $SrFe_{0.8}Ti_{0.2}O_{3-\delta}$, where several extra peaks appear in the XRD patterns. The observed behavior well corresponds to the literature data [9], showing formation of a superstructure in the cation-stoichiometric $SrFe_{1-x}Ti_xO_{3-\delta}$ ($x \geq 0.60$) due to ordering in the oxygen sublattice. Therefore, creation of minor A-site deficiency in Sr(Fe,Ti)$O_{3-\delta}$-based perovskites is likely to increase the structural disorder and to suppress oxygen-vacancy ordering. This may result from local inhomogeneities, such as lattice distortions near cation vacancies, statistically distributed in the structure. Such an assumption is in agreement with the data on ionic conduction in the A-site-deficient phases, discussed below.

The perovskite unit cell parameter (a) of $Sr_{0.97}Fe_{1-x}Ti_xO_{3-\delta}$ increases with the titanium concentration (Fig. 1), resembling the dependence observed for $SrCo_{1-x}Ti_xO_{3-\delta}$ [28, 29]. The cell enlargement may be associated with the presence of a significant fraction of Fe^{4+} cations, lower coordination numbers of Fe^{3+} with respect to Ti^{4+}, and/or a greater level of structural disorder when titanium is introduced in the lattice. The radius of octahedrally coordinated Ti^{4+} cations is smaller that that of high-spin Fe^{3+} in the same coordination [30]. However, the size of Ti^{4+} may be larger if the coordination number of titanium is higher with respect to Fe^{3+} or when the average oxidation state of iron ions exceeds 3+ [30]. Note also that tetrahedrally coordinated Fe^{3+} cations may reside in oxygen vacancy-ordered microdomains, as reported for strontium ferrite [10]. Extensive formation of such microdomains should favor cell contraction, whereas statistically distributed

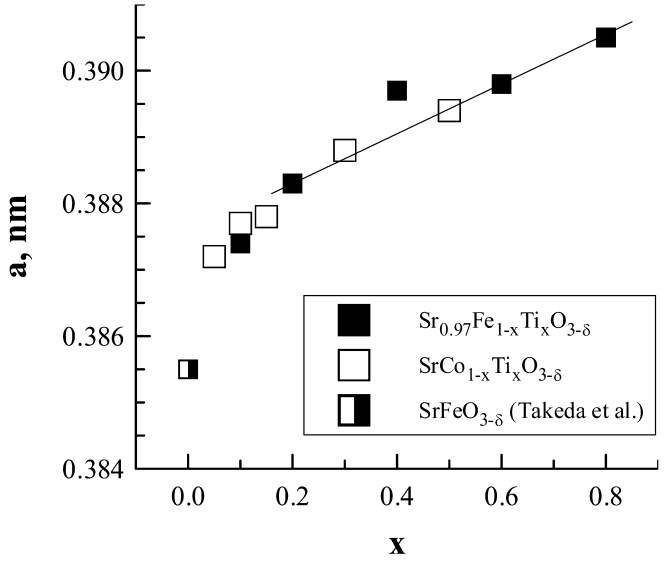

Fig. 1. Composition dependence of the cubic perovskite unit cell parameter in the $Sr_{0.97}Fe_{1-x}Ti_xO_{3-\delta}$ system. The data on $SrCo_{1-x}Ti_xO_{3-\delta}$ [28, 29] and the cubic $SrFeO_{3-\delta}$ phase [11] are shown for comparison. The error in the lattice parameter determination is ±0.0001 nm

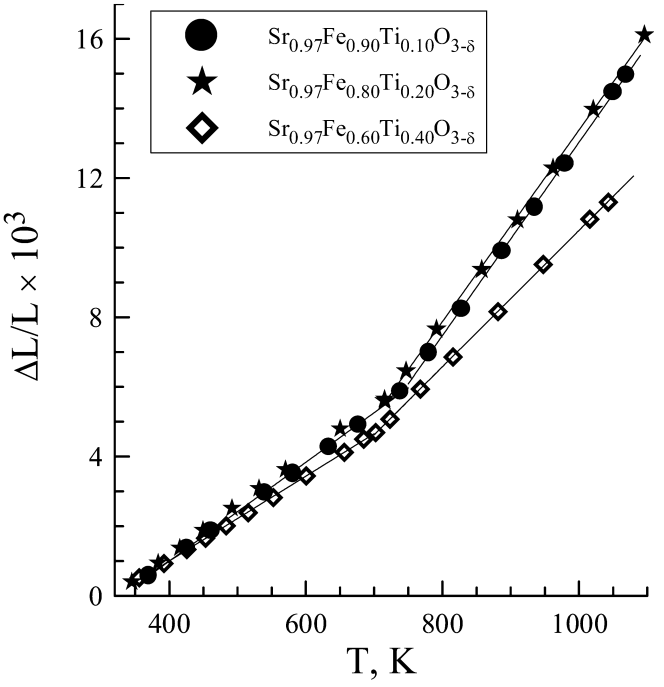

Fig. 2. Examples of dilatometric curves for $Sr_{0.97}Ti_{1-x}Fe_xO_{3-\delta}$ ceramics in air

oxygen-titanium octahedra are expected to increase the level of disorder and, hence, the unit cell volume. This hypothesis is confirmed by significant nonlinearity of the lattice parameter versus composition in the Fe-rich range (Fig. 1), as well as earlier reports [9].

In the system $Sr_{1-y}Fe_{0.8}Ti_{0.2}O_{3-\delta}$, the perovskite cell volume increases with increasing A-site vacancy concentration (Table 1). The main reason for such behavior refers, obviously, to the coulombic anion repulsion [31]. However, increasing lattice disorder due to randomly distributed cation vacancies, mentioned above, may also contribute to the unit cell enlargement. Detailed TEM studies, focused on revealing the types of ordering in the oxygen sublattice of A-site-deficient phases, are now in progress.

Thermal expansion and stability in a CO_2 atmosphere

An example of dilatometric curves, typical for $Sr_{1-y}Ti_{1-x}Fe_xO_{3-\delta}$ ceramics in air, is given in Fig. 2. In the low-temperature range (300–750 K), the average linear thermal expansion coefficients (TECs) vary from 11.7×10^{-6} to 16.5×10^{-6} K^{-1}. Further increase in temperature leads to a greater thermal expansion coefficient, associated with oxygen losses, and probably also partial disordering on heating [7, 8, 11]. The TEC values at 750–1050 K are as high as $(16.6–31.1)\times10^{-6}$ K^{-1}.

The thermal expansion of $Sr_{1-y}Fe_{1-x}Ti_xO_{3-\delta}$ was found to increase with A-site deficiency and to decrease with titanium additions (Fig. 3). The former phenomenon represents the well-known effect of vacancies in a crystal lattice, increasing anharmonicity of atomic vibrations (for instance, see [31, 32]). The increase in TEC values with y may also be contributed by increasing oxygen-vacancy concentration, which is the most likely charge compensation mechanism, as discussed below. Lower thermal expansion of the materials with higher titanium content is due to smaller oxygen losses on heating, since Ti^{4+} cations under the studied conditions have a constant oxidation state.

Figure 4 presents selected IR absorption spectra of $Sr_{1-y}Fe_{0.8}Ti_{0.2}O_{3-\delta}$ powders, annealed at 1270 K and then slowly cooled in CO_2-purified air, prior to exposure to a CO_2 atmosphere for 40–50 h, at 298 or 473 K. For A-site stoichiometric $SrFe_{0.8}Ti_{0.2}O_{3-\delta}$, keeping in CO_2 leads to the appearance of IR bands characteristic of $SrCO_3$ [33], clearly indicating surface decomposition of the perovskite phase (Fig. 4A). Heating up to 473 K increases the reaction rate, probably due to kinetic

Table 1. Unit cell parameters and activation energies for the total electrical conductivity of $Sr_{1-y}Fe_{0.80}Ti_{0.20}O_{3-\delta}$

y	a (nm) (±0.0001 nm)[a]	T (K)	E_a (kJ/mol)[a]	ln A_0 (S K/cm)[a]
0.01	0.3882	360–670	18 ± 2	13.7 ± 0.4
0.03	0.3883	300–720	21.2 ± 0.9	13.7 ± 0.3
0.06	0.3896	490–730	25 ± 2	14.0 ± 0.4

[a]Note that a is the parameter for the cubic perovskite unit cell at room temperature. E_a and A_0 are the activation energy and pre-exponential factor, calculated in the given temperature range as $\sigma = (A_0/T)\exp(-E_a/RT)$

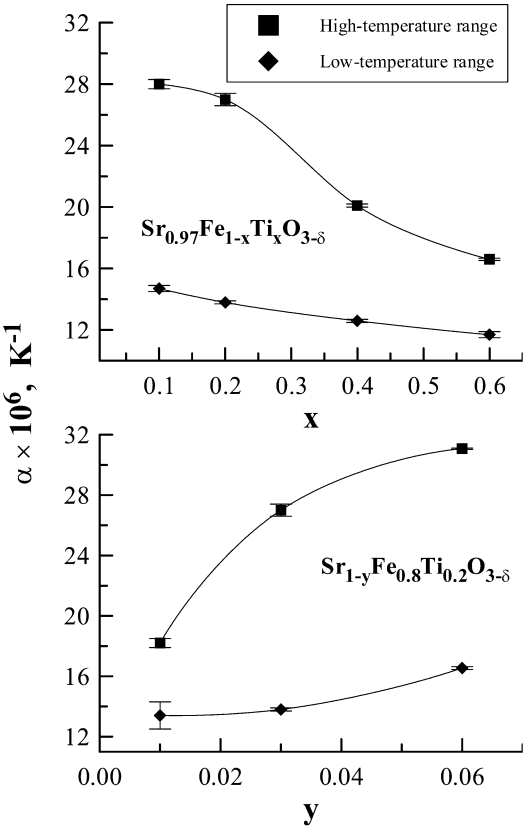

Fig. 3. Composition dependence of the average thermal expansion coefficients for $Sr_{1-y}Fe_{1-x}Ti_xO_{3-\delta}$ ceramics in air

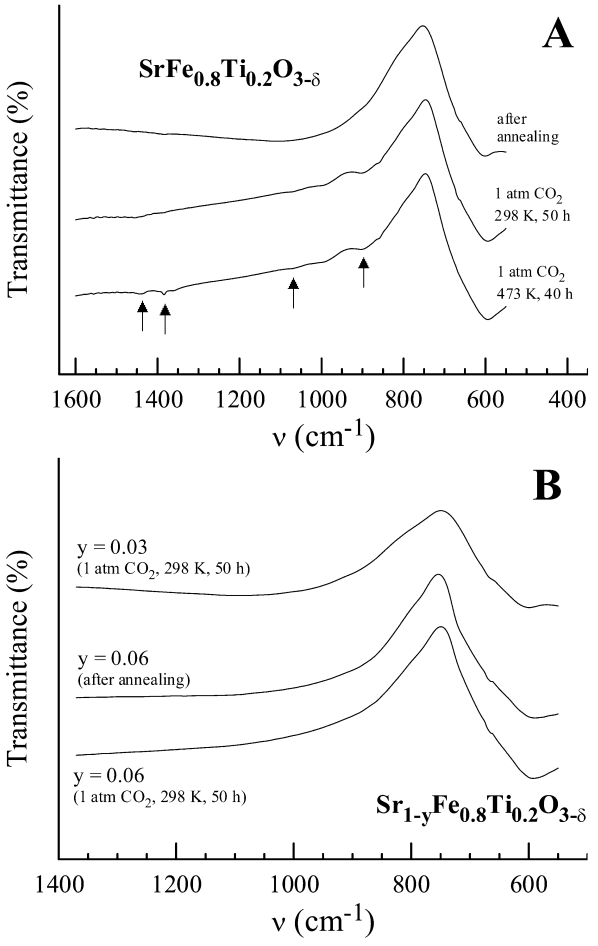

Fig. 4A, B. IR absorption spectra of $Sr_{1-y}Fe_{0.80}Ti_{0.20}O_{3-\delta}$ phases at room temperature, obtained after annealing in CO_2-free air at 1270 K for 2 h, with subsequent slow cooling and keeping in a CO_2 atmosphere. *Arrows* show peaks characteristic of the $SrCO_3$ phase [33]

stagnation at room temperature. Similar results were obtained for $Sr_{0.99}Fe_{0.8}Ti_{0.2}O_{3-\delta}$. As expected, higher A-site deficiency suppresses formation of strontium carbonate owing to the lower thermodynamic activity of Sr in the perovskite phases; no traces of $SrCO_3$ were observed in the case of $Sr_{1-y}Fe_{0.8}Ti_{0.2}O_{3-\delta}$ ($y = 0.03$–0.06) reacted under the same conditions (Fig. 4B). These results clearly demonstrate an improvement in the stability of the perovskites by creating A-site vacancies.

Total conductivity

Temperature dependence of the total electrical conductivity of the title materials in air is presented in Fig. 5. Numerous literature data [7, 8, 9] show that the conductivity is predominantly p-type electronic. Indeed, the oxygen ion transference numbers in air do not exceed 0.02 (Table 2 and Fig. 6). At 650–850 K, all studied phases exhibit a transition to a pseudo-metallic behavior, which is typical for $SrFeO_{3-\delta}$-based materials [7, 8, 9] and is related both to oxygen losses on heating and partial delocalization of the electronic charge carriers [15]. Increasing the titanium content in $Sr_{0.97}Fe_{1-x}Ti_xO_{3-\delta}$ leads to lower p-type conductivity, while the activation energy for the electron-hole conduction increases (Fig. 7A). This results from decreasing concentrations of mobile charge carriers (Fe^{4+}) and Fe-O-Fe bonds, providing electronic transport in perovskites. A similar behavior is observed on increasing the cation deficiency in the A sublattice at temperatures below 700 K (Fig. 5). When vacancies are created in the strontium sites, the crystal electroneutrality condition requires either increasing oxygen nonstoichiometry or formation of Fe^{4+}. In the latter case, the electron-hole conductivity would increase. Hence, the charge compensation of the A-site deficiency occurs mainly via oxygen vacancy formation.

Ionic conduction: effect of A-site deficiency

When discussing the data on ionic conduction, it should be emphasized that the presence of non-negligible surface exchange limitations to oxygen transport is typical for most ceramic materials based on $AMO_{3-\delta}$ (A = Sr, Ca; M = Fe, Co) [14, 15, 22, 26, 27, 28]. As a result, the values of the ion transference numbers and ionic conductivity, obtained from the OP and FE measurements, may be underestimated [26]. In the case of the FE method, catalytically active porous platinum electrodes may promote oxygen exchange, thus decreasing the limiting role of membrane surface exchange [26]. This

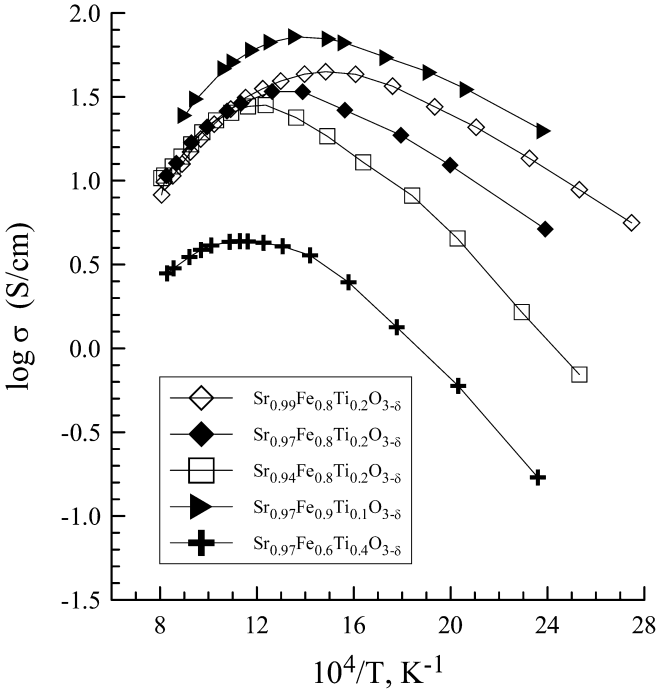

Fig. 5. Temperature dependence of the total electrical conductivity of $SrFeO_{3-\delta}$-based solid solutions in air

technique was thus chosen for the study of ionic conduction as a function of A-site deficiency. Nevertheless, the ion transference numbers of the title materials, evaluated by the FE and OP methods, are quite close to each other (Table 2), which indicates that the effect of surface reactions is rather small. Therefore, taking into account the well-known correlation between bulk oxygen diffusion and surface exchange [35], one can expect that the trends in ionic conduction reported in this work reflect the true behavior of the perovskite phases.

Increasing the A-site cation vacancy concentration from 1 to 3% leads to an increase in the oxygen ionic conductivity of $Sr_{1-y}Fe_{0.80}Ti_{0.20}O_{3-\delta}$ ceramics by 2–2.5 times (Fig. 6). This effect might be partly related to the increase in the oxygen nonstoichimetry as a result of the cation vacancy charge compensation. However, the variation of y in the range 0.01–0.03 only changes the oxygen vacancy concentration by few percent. Hence, the higher ionic conductivity of $Sr_{0.97}Fe_{0.80}Ti_{0.20}O_{3-\delta}$ is attributed mainly to increasing structural disorder when the A-site deficiency increases, in agreement with XRD data. One possible reason may relate to local structure distortions, such as the tungsten bronze-type distortions [36], near the cation vacancies. Although these lattice defects should reduce the mobility of neighboring oxygen ions and vacancies, their random distribution in the perovskite-type lattice might suppress long-range ordering. However, when the A-site vacancy concentration is excessive, the total ionic conductivity may decrease, as found on comparing the results for $Sr_{0.94}Fe_{0.80}Ti_{0.20}O_{3-\delta}$ and $Sr_{0.97}Fe_{0.80}Ti_{0.20}O_{3-\delta}$ (Fig. 6). This trend is similar to the behavior of lanthanum-strontium cobaltites and aluminates [20, 22], even for

Table 2. Oxygen ion transference numbers for $SrFeO_{3-\delta}$-based perovskites at 1223 K in air, estimated from the faradaic efficiency (FE) and oxygen permeability (OP) results

Composition	Measurement method	t_o
$Sr_{0.97}Fe_{0.90}Ti_{0.10}O_{3-\delta}$	FE	4.1×10^{-3}
	OP	3.1×10^{-3}
$Sr_{0.99}Fe_{0.80}Ti_{0.20}O_{3-\delta}$	FE	5.5×10^{-3}
$Sr_{0.97}Fe_{0.80}Ti_{0.20}O_{3-\delta}$	FE	14.2×10^{-3}
	OP	15.3×10^{-3}
$Sr_{0.94}Fe_{0.80}Ti_{0.20}O_{3-\delta}$	FE	10.2×10^{-3}
$Sr_{0.97}Fe_{0.60}Ti_{0.40}O_{3-\delta}$	FE	28.8×10^{-3}
	OP	26.9×10^{-3}

cases when the tendency to partial ordering is considerably smaller than that in strontium ferrite. In the case of A-site-deficient lanthanum aluminate, such a behavior was ascribed to clustering of the cation and anion vacancies [20]. These clusters may indeed represent another type of lattice defect, statistical distribution of which may prevent partial ordering. The relationships between A-site deficiency and ionic conductivity in gallate-based materials [19, 21] are more complicated, possibly due to secondary phase formation.

Ionic conductivity versus B-site cation composition

The composition dependence of the specific oxygen permeability for the materials with a fixed Sr deficiency,

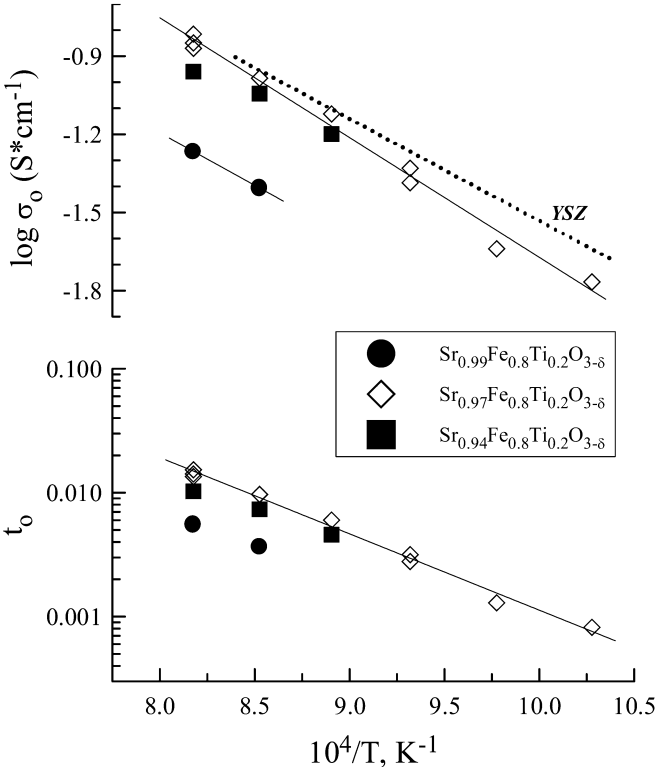

Fig. 6. Temperature dependence of the oxygen ionic conductivity and ion transference numbers of A-site-deficient $Sr_{1-y}Fe_{0.80}Ti_{0.20}O_{3-\delta}$ in air. The data on the conductivity of the $Zr_{0.92}Y_{0.08}O_{1.96}$ (YSZ) solid electrolyte [34] are shown for comparison

$Sr_{0.97}Fe_{1-x}Ti_xO_{3-\delta}$, is presented in Fig. 7B. The specific oxygen permeability $J(O_2)$ was extracted from the steady oxygen permeation fluxes (j) and the oxygen chemical potential gradient, normalized to the membrane thickness d, as follows [37]:

$$j = \frac{J(O_2)}{d} \ln\left(\frac{p_2}{p_1}\right) \quad (1)$$

where p_1 and p_2 are the oxygen partial pressures at the membrane permeate and feed sides, respectively ($p_1 < p_2$). As for the system $SrCo_{1-x}Ti_xO_{3-\delta}$ [28, 29], the oxygen permeability and ionic conductivity of $Sr_{0.97}Fe_{1-x}Ti_xO_{3-\delta}$ ($x \geq 0.20$) monotonically decrease with titanium additions owing to decreasing oxygen vacancy concentration (Fig. 7B). In this range of x, the activation energy for ionic transport is essentially independent of composition (Fig. 7A). On the other hand, decreasing x down to 0.10 leads to a greater activation energy and considerably lower ionic conductivity. This unambiguously suggests that substitution of 20% iron with titanium suppresses the ordering of oxygen vacancies and stabilizes the cubic perovskite lattice of strontium ferrite, in agreement with the literature on $SrFeO_{3-\delta}$-based phases [9, 13]. Analogously to the effect of A-site vacancies, random distribution of oxygen-titanium octahedra is likely to prevent long-range ordering in the lattice.

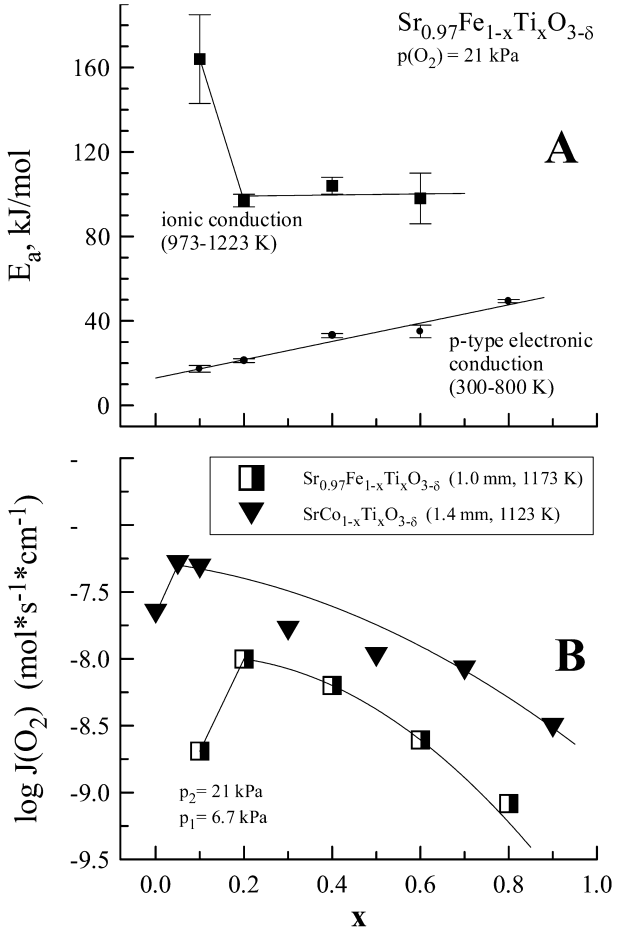

Fig. 7. **A** Composition dependence of the activation energies for the ionic and electronic conductivities in air, and **B** the specific oxygen permeability of $Sr_{0.97}Fe_{1-x}Ti_xO_{3-\delta}$ membranes. The data on $SrCo_{1-x}Ti_xO_{3-\delta}$ membranes [28, 29] are shown for comparison

Time degradation of oxygen transport

As found in our previous work [15, 26], $Sr(Fe,Ti)O_{3-\delta}$ membranes exhibit an extremely prolonged transient regime after placement under an oxygen chemical potential gradient at 970–1220 K. The oxygen permeation fluxes typically decrease by 2–10 times before steady state, and the stabilization time is as long as 100–700 h. Figure 8 presents a typical example of the transient processes for $Sr_{0.97}Fe_{0.90}Ti_{0.10}O_{3-\delta}$ membranes. The stabilization time increases with increasing iron content [15, 26]. Such a transient regime has been associated with the formation of vacancy-ordered microdomains [15], typical for strontium ferrite.

Results reported for $Sr(Co,Ti)O_{3-\delta}$ ceramics [28] showed that time degradation of the oxygen permeability can be prevented by a slow cycling of the oxygen partial pressure at the membrane permeate side. As ordering in the oxygen sublattice is more extensive at reduced oxygen pressures [10] and occurs with a finite rate, periodic variations in the oxygen nonstoichiometry are expected to partially suppress microdomain formation. A series of experiments with $Sr_{0.97}(Fe,Ti)O_{3-\delta}$ membranes confirmed that this is also true for strontium titanate-ferrite ceramics. Cycling of the oxygen pressure was found to accelerate steady-state achievement and, in some cases, to result in higher permeation fluxes. A representative

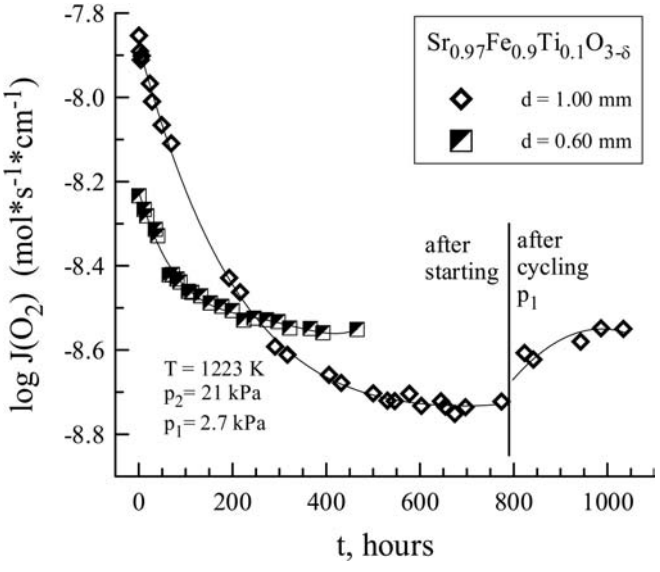

Fig. 8. Time dependence of the oxygen permeability of $Sr_{0.97}Fe_{0.90}Ti_{0.10}O_{3-\delta}$ ceramics after placing the membranes under a fixed oxygen chemical potential gradient. For the steady regime, the accuracy of keeping p_1 constant was ± 0.3 kPa. The increase in the permeability was observed after cycling p_1 from 2.0 to 17.5 kPa during 24 h

example is given in Fig. 8, for a $Sr_{0.97}Fe_{0.90}Ti_{0.10}O_{3-\delta}$ membrane with a thickness of 1.0 mm, kept under a fixed oxygen pressure gradient (21/2.7 kPa) for 700 h. The steady-state permeation flux is about 8 times lower than its starting value. However, subsequent cycling of p_1 in the range from 2.0 to 17.5 kPa during 24 h increased the flux by about 60%, and no further degradation was detected for 250 h, after cycling. Although the observed phenomenon is quite complex, these results show a possibility to prevent the membrane degradation with time by using a non-steady operation regime.

Conclusions

Dense single-phase $Sr_{1-y}Fe_{1-x}Ti_xO_{3-\delta}$ ($x = 0.10$–0.60, $y = 0$–0.06) ceramics were prepared by a standard solid-state synthesis route and characterized using XRD, IR absorption spectroscopy, SEM/EDS, dilatometry, and measurements of electrical conductivity, oxygen permeability, and faradaic efficiency. A-site deficiency and doping with titanium both lead to an increasing unit cell volume. The average TECs of $Sr_{1-y}Ti_{1-x}Fe_xO_{3-\delta}$ in air vary in the range $(11.7–16.5)\times10^{-6}$ K^{-1} at temperatures below 750 K and $(16.6–31.1)\times10^{-6}$ K^{-1} in the range 750–1100 K. The TEC values increase with A-site deficiency, whilst incorporation of titanium in the B sites has the opposite effect. IR spectra show a significant enhancement in stability of the perovskite phases in a CO_2 atmosphere when even 1% cation vacancies are created in the A sublattice.

The total electrical conductivity of $Sr_{1-y}Fe_{0.80}Ti_{0.20}O_{3-\delta}$, predominantly p-type electronic, decreases with increasing A-site deficiency in the temperature range 300–700 K and is essentially independent of the A-site deficiency at higher temperatures. This suggests a charge compensation mechanism via increasing oxygen nonstoichiometry. The ionic conductivity considerably increases with the cation vacancy concentration up to $y = 0.03$, probably due to greater structural disorder and also higher oxygen-vacancy content. Incorporation of moderate amounts of titanium in $Sr_{0.97}Fe_{1-x}Ti_xO_{3-\delta}$ (up to 20%) also suppresses ordering in the oxygen sublattice, which results in a higher ionic conductivity and a lower activation energy for ionic transport. For $x > 0.20$, ionic and p-type electronic conductivities both decrease with Ti additions. Time degradation of the oxygen permeation fluxes can be reduced by cycling of the oxygen pressure at the membrane permeate side.

Acknowledgements Financial support from the FCT, Portugal (projects Praxis/CTM/14170/1998 and BD/6827/2001), INTAS (project 00276), the Belarus Ministry of Education and Science, and the Belarus State Program for Basic Research "Matter-2" is gratefully acknowledged.

References

1. Pena MA, Fierro JLG (2001) Chem Rev 101:1981
2. Islam MS (2000) J Mater Chem 10:1027
3. Alcock CB, Doshi RC, Shen Y (1992) Solid State Ionics 51:281
4. Yamamoto O (2000) Electrochim Acta 45:2423
5. Mazanec TJ, Cable TL, Frye JG, Kliewer WR (1997) US Patent 5591315
6. Schwartz M, White J, Sammels A (1997) Int Patent Application PCT WO 97-41060
7. Kaus I, Anderson HU (2000) Solid State Ionics 129:189
8. Poulsen FW, Lauvstad G, Tunold R (1994) Solid State Ionics 72:47
9. Steinsvik S, Bugge R, Gjonnes J, Tafto J, Norby T (1997) J Phys Chem Solids 58:969
10. Grenier J-C, Pouchard NEM, Hagenmuller P (1985) J Solid State Chem 58:243
11. Takeda Y, Kanno K, Takada T, Yamamoto O, Takano M, Nakayama N, Bando Y (1986) J Solid State Chem 63:237
12. Hodges JP, Short S, Jorgensen JD, Xiong X, Dabrowski B, Mini SM, Kimball CW (2000) J Solid State Chem 151:190
13. Mazanec TJ (1997) Electropox gas reforming. In: Anderson HU, Krandhar AC, Liu M (eds) Ceramic membranes I. Electrochemical Society, Pennington, NJ, pp 16–28
14. Kharton VV, Viskup AP, Kovalevsky AV, Jurado JR, Naumovich EN, Vecher AA, Frade JR (2000) Solid State Ionics 133:57
15. Kharton VV, Kovalevsky AV, Viskup AP, Jurado JR, Figueiredo FM, Naumovich EN, Frade JR (2001) J Solid State Chem 156:437
16. Carolan MF, Dyer PN, LaBar JM, Thorogood RM (1993) US Patent 5261932
17. Carolan MF, Dyer PN, Motika SA, Alba PB, (1998) US Patent 5712220
18. Jurado JR, Figueiredo FM, Charbage B, Frade JR (1999) Solid State Ionics 118:89
19. Stevenson JW, Armstrong TR, Pederson LR, Li J, Lewinsohn CA, Baskaran S (1998) Solid State Ionics 113–115:571
20. Nguyen TL, Dokiya M, Wang S, Tagawa H, Hashimoto T (2000) Solid State Ionics 130:229
21. Ahmad-Khanlou A, Tietz F, Stover D (2000) Solid State Ionics 135:543
22. Kovalevsky AV, Kharton VV, Tikhonovich VN, Naumovich EN, Tonoyan AA, Reut OP, Boginsky LS (1998) Mater Sci Eng B 52:105
23. Kharton VV, Zhuk PP, Tonoyan AA, Zhabko TE, Vecher AA (1991) Inorg Mater 27:2240
24. Tikhonovich VN, Kharton VV, Naumovich EN, Savitsky AA (1998) Solid State Ionics 106:197
25. Berenov AV, MacManus-Driscoll JL, Kilner JA (1999) Solid State Ionics 122:41
26. Kharton VV, Viskup AP, Kovalevsky AV, Figueiredo FM, Jurado JR, Yaremchenko AA, Naumovich EN, Frade JR (2000) J Mater Chem 10:1161
27. Kharton VV, Figueiredo FM, Kovalevsky AV, Viskup AP, Naumovich EN, Jurado JR, Frade JR (2000) Defect Diffusion Forum 186–187:119
28. Kharton VV, Shuangbao Li, Kovalevsky AV, Naumovich EN (1997) Solid State Ionics 96:141
29. Kharton VV, Shuangbao Li, Kovalevsky AV, Viskup AP, Naumovich EN, Tonoyan AA (1998) Mater Chem Phys 53:6
30. Shannon RD (1976) Acta Crystallogr Sect A 32:751
31. West AR (1984) Solid state chemistry and its applications. Wiley, New York
32. Hayashi H, Inaba H, Matsuyama M, Lan NG, Dokiya M, Tagawa H (1999) Solid State Ionics 122:1
33. Nyquist RA, Kagel RO (1997) Handbook of infrared and Raman spectra of inorganic compounds and organic salts, vol. 4: IR spectra of inorganic compounds. Academic Press, San Diego
34. Badwal SP (1992) Solid State Ionics 52:23
35. Steele BCH (1995) Solid State Ionics 75:157
36. Slater PR, Irvine JTS (1999) Solid State Ionics 120:125
37. Moebius H-H (1986) Oxygen current density coefficient of oxidic materials. In: Extended abstracts, 37th ISE meeting, vol. 1. Vilnius, pp 136–139